

2003

Towards a single-mode dispensed polymer optical waveguide

Jill Michelle Kalajian
University of South Florida

Follow this and additional works at: <http://scholarcommons.usf.edu/etd>

 Part of the [American Studies Commons](#)

Scholar Commons Citation

Kalajian, Jill Michelle, "Towards a single-mode dispensed polymer optical waveguide" (2003). *Graduate Theses and Dissertations*.
<http://scholarcommons.usf.edu/etd/1402>

This Thesis is brought to you for free and open access by the Graduate School at Scholar Commons. It has been accepted for inclusion in Graduate Theses and Dissertations by an authorized administrator of Scholar Commons. For more information, please contact scholarcommons@usf.edu.

TOWARDS A SINGLE-MODE DISPENSED POLYMER OPTICAL WAVEGUIDE

BY

JILL MICHELLE KALAJIAN

A thesis submitted in partial fulfillment
of the requirements for the degree of
Masters of Science
Department of Physics
College of Arts and Sciences
University of South Florida

Major Professor: Nicholas Djeu, Ph.D.
Dennis K. Killinger, Ph.D.
Myung K. Kim, Ph.D.

Date of Approval:
November 19, 2003

Keywords: Waveguides, Photonics, Optics, Telecommunications, Polymer

© Copyright 2003, Jill Michelle Kalajian

To Mom, Thanks

Acknowledgments

I would like to thank my advisor Dr. Nicholas Djeu

Table of Contents

List of Figures	ii
List of Tables	iii
Abstract	iv
Chapter One Introduction	1
Chapter Two Methods of Waveguide Fabrication	5
2.1 Waveguide Fabrication In a Polymer By an Electron Beam	6
2.2 Injection-molding	6
2.3 UV Written Waveguides	8
2.4 Dispensed polymer waveguides	9
2.5 Doping of Polymers To Create Optical Waveguide Devices	11
Chapter Three Fabrication of the Waveguides	12
3.1 Equipment and Setup	12
3.2 Polymer	15
3.3 Fabrication of the waveguides	20
Chapter Four Results and Calculation	24
4.1 Waveguide Characterization	24
4.2 The Effective Index of Refraction	28
4.2.1 Theory and Derivation of Index of Refraction Equations for TE modes	28
4.2.2 Calculations of the Parabolic Profile Graded Index of Refraction	31
4.2.3 Calculations for the TM modes	35
4.3 Single mode waveguide determination	35
4.3.1 Theory for Determining the Number of Modes	36
4.3.2 Calculation of wavelengths that have only one mode	38
4.4 Results for claddings with a different index	41
4.5 Spot Size Calculations	43
Chapter Five Conclusion	46
5.1 Summary	46
5.2 Future Work	47
References	48
Appendices	50

List of Figures

Figure 1.	Dispensed Polymer Set up	13
Figure 2.	Tip of Biological Pipette	14
Figure 3.	Diagram of the wetting angle θ	17
Figure 4.	SEM Photo of Dispensed Polymer Waveguide	25
Figure 5.	AFM 3-D Profile of Dispensed Polymer Waveguide	26
Figure 6.	AFM Profile Data with Nonlinear Least Squares Fit to Circle Equation	27
Figure 7.	Planer Waveguide Coordinate system	29
Figure 8.	Mode Cutoff for $n = 1.48$	32
Figure 9.	Parabolic Fit to Effective Index of Refraction Data for $\lambda = 1.50\mu$	34
Figure 10.	Helical Path of Ray In a Fiber	37
Figure 11.	$2\int k_r dr$ vs. λ - for $l = 0$; Region of Only One Mode	40
Figure 12.	$2\int k_r dr$ vs. λ - for $l = 1$; Regions With No Modes at $l = 0$	42
Figure 13.	Spot Sizes in both the x, squares, and y, circles, axis	45

List of Tables

Table 1: Drop width to height measurements

19

TOWARDS A SINGLE-MODE DISPENSED POLYMER OPTICAL WAVEGUIDE

JILL M. KALAJIAN

ABSTRACT

Dispensed organic polymer optical waveguides suitable for single-mode operation were recently fabricated. Different dispensing pressures, polymers, and dispensing tips were used in the drawing method.

The waveguides were measured to be approximately 16μ wide and 0.8μ tall. This is significantly smaller than previously reported dimensions of 300μ x 3.5μ waveguides fabricated with a similar dispensed polymer method. The waveguides were also found to be suitable for single-mode operation through a series of approximate calculations. This is also something previously not achieved with the larger waveguides.

This novel approach to waveguide fabrication could reduce the expense and time of creating single mode waveguides for rapid development applications. It will also allow the waveguides to be fabricated to be flexible as well as doped to be active devices.

CHAPTER ONE

INTRODUCTION

Since the development of lasers and optoelectronics the telecommunications industry has driven the rise of the new field of photonics. Waveguides allow the light from these devices to travel large distances without being obstructed and to be directed easily in small areas without the need for complicated prism, lens and mirror systems.

Waveguides on surfaces are needed for active devices on substrates as well as interconnects for photonic integrated circuits. Innovative ways to create these waveguides on various substrates have been investigated for many years. Dispensed polymer waveguides have shown promise for this application. They have the advantage of being inexpensive and easy to create as well as being versatile in the makeup of the polymer to achieve a variety of optical properties.

Telecommunications has traditionally used fibers between different elements of networks such as between a laser and a beam splitter. This is akin to the original computers that were hard wired between each element. The advent of the integrated circuit board meant a savings of space and money. Waveguides on a substrate are a similar solution for photonics. The number of elements in a given area is limited only by the width of the waveguides and the

size of the elements themselves. Once the method of fabrication is developed the waveguides can also serve as active devices, such as optical amplifiers needed within an optical system.¹

Optical fibers consist of a core of dielectric material surrounded by a medium with a lower index of refraction. These fibers, depending on the size, shape and composition, can be either multimode or single-mode. Modes are fields that maintain the same transverse distribution and polarization at all points along the fiber axis. Multimode fibers support, as the name suggests, more than one mode in the electric field. Different modes have different propagation constants and group velocities. Those fibers have the disadvantage of pulse spreading of the light as it travels down the fiber caused by the differences in the group velocities, although this is reduced in fibers with a graded index of refraction. When a fiber only allows one mode the fiber is referred to as single-mode. These fibers minimize the effect of pulse spreading, and are preferred for long haul applications.¹ Single-mode waveguides are better suited to telecommunications applications because coupling to single-mode fibers are more efficient. Multimode devices between single-mode fibers have much higher losses due to the change in the shape of the modes. However, single-mode waveguides require the core of the waveguide to be sufficiently small. This has been an obstacle in the past for producing single mode waveguides with the dispensed polymer technique.

Active devices, such as amplifiers, optical modulators, and lasers can also be fabricated using single-mode waveguides. Such devices are used, for

example, to amplify a signal along a telecommunications path by having dopants in the waveguide, which can be excited. These excited atoms or molecules would then act as an optical amplifier for a beam traveling within the waveguide.² These waveguide optical amplifiers will be even more effective in data communications, compared to the telecommunications industry, where the distances are small while the relative complexity is increased.³

Devices fabricated with polymers have many advantages over their crystalline or glass counterparts. First, polymers have a low dispersion in the index of refraction at telecommunication wavelengths. Another advantage of polymers is the wide range of materials they can be deposited onto. Polymers will adhere to many substrates including semiconductors. Also polymers can be easily integrated into optical circuits that include other optical materials. This includes fabricating vertical waveguides to interconnect multiple layers in optical integration.²

For this thesis, polymer waveguides were fabricated using a UV curable polymer dispensed from a biological micropipette. A variety of combinations of polymers, micropipettes, and fabrication techniques were investigated. The objective of the project was to produce a waveguide with a smaller core than waveguides previously produced in this fashion. These smaller waveguides can be made single-mode, and leave open the future possibility of being used to create active devices with the addition of dopants to the polymer.

Chapter Two will present background information on several methods of waveguide fabrication including the dispensed polymer technique. Also, previous work with active devices in polymer will be discussed.

Chapter Three will begin with an explanation of the setup and equipment used in the research for this thesis project. A discussion of the polymers and their properties is included as well. Finally the procedures used to fabricate the waveguides will be described.

Chapter Four will report the physical measurements of the resulting waveguides. Theories of planar waveguides and optical fibers with parabolic index profile will be reviewed, and applied to the polymer waveguide to show that it can be made into a single mode device.

Chapter Five will summarize the significance of this project and include suggestions for further investigation and future work.

CHAPTER TWO

METHODS OF WAVEGUIDE FABRICATION

Polymer waveguides are of interest in the field of optoelectronics. They constitute one means of providing interconnections between elements of optoelectronic integrated circuits. Some of the methods for fabricating polymer waveguides include reactive ion etching, chemical etching, injection molding, electron beam irradiation, and pressure dispensing. Many of these methods are expensive and time consuming and would limit the rapid development and testing of new materials and devices. Also, fabrication methods are needed that result in single-mode waveguides for active device applications. Polymers, in addition to the ease of shaping, offer a great deal of control in the structure, size and composition for these devices. For example, the substrate for these devices could even be adapted to give flexible waveguides to further minimize the space taken up by an active device. A highly polished thin flexible ribbon of polymer for the substrate would take advantage of the flexibility of the core and cladding to create a waveguide that could be wound around itself to take up less space.

2.1 Waveguide Fabrication In a Polymer By an Electron Beam

One technique, shown by Darraud-Taupiac, for fabrication of waveguides in a polymer substrate is bombardment by an electron beam.⁴ A highly transparent polymer, such as poly(diethylene glycol bis(allylcarbonate)), a PMMA polymer, is used as the substrate. The polymer is coated with a 20 nanometer thick Au-Pd layer to keep the electron beam from charging the polymer. A 10 x 10 x 1 mm section of the polymer substrate is then irradiated using a scanning electron microscope. Energies in the range of 10 – 30 keV are typically used, allowing the electron beam to penetrate up to about 10 microns. The section of polymer substrate that is irradiated has an increased index of refraction compared to the unexposed area. This produces single-mode or multimode graded index waveguides based on the thickness of the waveguide.

While the losses had not yet been determined, values of about 2dB/cm are expected. The scanning electron microscope needed to produce these waveguides makes this technique costly. Finally, the waveguides are also relatively large for use in photonic integrated circuits.

2.2 Injection-molding

Single-mode polymer waveguides with low transmission losses can be fabricated using injection-molding technology. In a publication by Neyer et al. a method of this process is described.⁵ The first step is conventional UV-light lithographic structuring of photo resist layers on silicon, with the thickness of the resist determining the thickness of the final waveguides. Development of the

photo resist results in the waveguide structure being transferred to the resist in the form of rectangular ridges. Electroplating the developed resist layers with nickel creates a metal mold that replicates the negative of the resist profile and will define the outline of the grooves in the device structure. This negative is then used as an insert in the injection-molding machine for the substrate. A polymer like polymethylmethacrylate, or PMMA, of high optical quality is then used as the injection molded material and creates the molded substrate polymer. The grooves left in the mold by the nickel profile are then filled with a waveguide core polymer like ethyleneglycoldimethacrylate or EGDMA. This core polymer is selected because it has a higher index of refraction than the substrate as well as not reacting with the substrate and dissolving it. Another layer of the substrate polymer is pressed on top to remove the excess liquid core polymer and become the cover of the waveguide. The waveguide is then cured using UV light.

The losses associated with this technique are 0.3 dB/cm at 1300nm. This is better than the previous method. This method also has the advantage of being easily mass-produced once the fabrication of the mold is finished. The core polymer could also be changed to achieve single-mode waveguides at different wavelengths. However there are disadvantages to this system. The process is not only time consuming, but also expensive during the research and development process.

2.3 *UV Written Waveguides*

UV written waveguides in polymers on silicon or silica is another frequent method of fabrication. In a recent report by Koo, et al., both the synthesis of the polymers and the UV writing technique to fabricate the waveguides are explained.⁶ Polymers developed for waveguide applications such as the PMMA are often used in this fabrication process. Synthesis of these polymers involves thermally initiated free radical polymerization at an elevated temperature and the resulting polymers are precipitated into ether. The esterification step then results in a pure white powder substance. This polymer is then dissolved in a solvent and filtered before it is used to spin-coat the substrate. The writing of the waveguides is done using a frequency-doubled argon ion laser with a 244 nm wavelength. The beam of the laser is focused in the polymer core layer, and the substrate and layer are moved on computer controlled translational stages to crosslink the polymer. The index of refraction is greater in the regions that the polymers have been crosslinked as compared to the regions not exposed to the UV beam. This method has the option of spin coating another layer on top of the UV written layer to place many layers of waveguides on top of each other.

The ability to change the polymers used in the substrates within the selection conditions mentioned previously makes this method more versatile. Desired optical properties could be achieved with simple substitution of one polymer for another. Although the layering of waveguides has many advantages in the development of a final extensive product, the development stage of any one project would be hindered by the expense of the frequency doubled argon

ion laser. The many steps involved also make this fabrication method time consuming. The losses are also higher for this waveguide fabrication method, being 0.4 - 0.9 dB/cm.

2.4 Dispensed polymer waveguides

Direct dispensed polymer waveguides on glass substrates have previously been fabricated with optical adhesives that have a higher index of refraction than glass. They are dispensed onto the substrate directly and cured immediately with no further processing required.

Keyworth, et al. produced both polymer surface waveguides and polymer V-groove waveguides in this manner.⁷ These early polymer surface waveguides were dispensed on a silicon substrate. Norland optical adhesive was used for its high index of refraction and the small amount of volume lost during curing under a UV light. The polymer was dispensed using a 160-micron inner-diameter syringe to form the core, and an inexpensive mercury light source was used for curing since there is no requirement for a small focused spot. As pressure dispenses polymer from the syringe a translation stage was moved beneath the tip to create the waveguide. These waveguides used air as the top cladding, although it was suggested that another polymer of lower index of refraction than the core could be placed on top of the waveguides.

Previously V-grooves were formed in a silicon wafer by anisotropic etching. Polymer was then poured on the surface and forced into the grooves with a rubber blade and the excess polymer was then removed with abrasive paper

that would cause minimal scratching. With the previously discussed dispensed polymer method the V-groove could be filled without wasting excess polymer or scratching the surface of the waveguides. It should be noted that losses were similar for the waveguides both with and without the scratches, which implies the losses are due to a mechanism other than scattering from the surface.⁷

The waveguides fabricated were measured with a profilometer and found to have a parabolic cross section. They were typically larger than 300 microns wide and 3.5 microns high. The waveguides were shown to behave as slab waveguide, with a graded index of refraction with a parabolic profile in the transverse direction. Although it was noted that single mode waveguides are theoretically possible, all waveguides fabricated by them were multimode.⁸

Compared to other fabrication methods, this technique requires much less expensive equipment for fabrication; however, these waveguides were multimode, and therefore less desirable for telecommunication uses. This technique also had the lowest losses of all the fabrication techniques. At 633 nm losses of approximately 0.2 dB/cm were determined for the V-groove waveguides and 0.45 dB/cm was found at 633 nm for the surface waveguides. These lower losses make this method a reasonable choice to improve upon. The fabrication method for this thesis project significantly reduces the size of the dispensed polymer waveguide. The smaller waveguides are better for photonic devices and are easily fabricated as single-mode waveguides.

2.5 Doping of Polymers To Create Optical Waveguide Devices

According to work done by Slooff, et al., polymer waveguides doped with rare-earth ions as the active element can be used for optical amplification.⁹ The trivalent ions such as Erbium (Er), Neodymium (Nd), Europium (Eu), and Terbium (Tb) are commonly used in optical applications. Er and Nd in particular are used as they have transitions at 1.53 and 1.34 microns respectively. Optical gain is achieved with these rare-earth ions by first exciting the ion from its ground state into a higher short-lived state. The ion quickly decays through non-radiating means to a longer-lived excited state. When it decays back to the ground state, a photon is released.

The Er salts are inorganic and cannot be directly dispersed into an organic polymer. First an organic liquid must encapsulate the Er^{+3} ions, and then the complex can be dispersed into the polymer film. A channel waveguide is fabricated with a high refractive index optical polymer doped with the Er^{+3} complexes and embedded in a low index polymer. When excited by a wavelength of 488 nm a gain of 1.7dB/cm was observed. This could be applied to create a no loss splitter with a waveguide only a few centimeters in length.⁹

The process to create the polymers with the inclusion of the dopants with this technique is very time consuming and difficult. However, once the polymer is doped conventional waveguide fabrication techniques may be employed.

CHAPTER THREE

FABRICATION OF THE WAVEGUIDES

3.1 Equipment and Setup

To fabricate the core of the waveguides for this project the very inexpensive setup shown in Figure 1 was used and photopolymers were drawn on fused silica glass substrates. The plunger of a 20 cubic centimeter glass syringe was secured at the 10cc line with sealing wax and approximately 2.5 meters of 32 gauge copper wire was wrapped around the vacant end. The wire wrapped end of the syringe was covered with a thermal insulating cloth in an attempt to retain heat from the current. Temperature in the syringe for drawing up or dispensing the polymer was controlled with a variable current source that was connected to the wire wrapped around the syringe.

A biological fertility assisted hatching micropipette from Humagen Fertility Diagnostics was secured into the tip of the syringe with sealing wax. The micropipette tip has an inner diameter of 9 – 10 microns and an outer diameter of 10 – 11 microns as shown in Figure 2. Humagen offers a wide range of micropipette tips. However, the assisted hatching micropipettes proved to be the easiest to work with. Partial Zona Dissection micropipettes were also used for some trials. These pipettes have a long thin taper with similar inner and outer

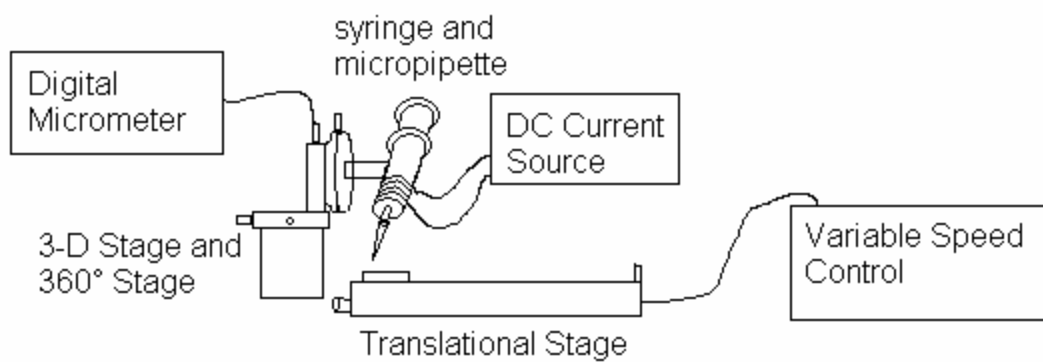


Figure 1: Diagram of Setup

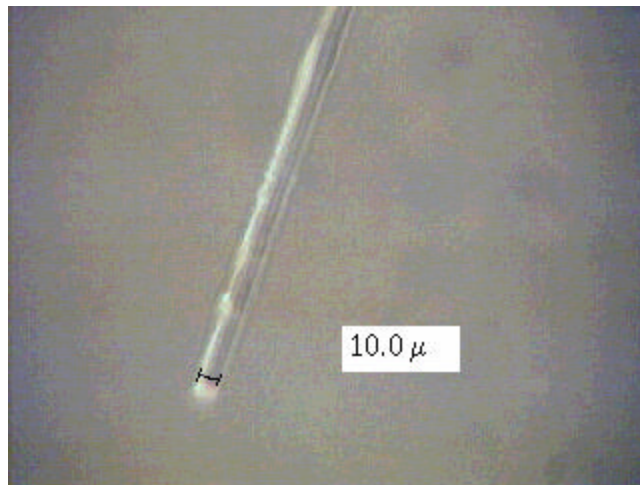


Figure 2: Example of the Pipette tip measured to be 10.0 μ outer diameter

dimensions to the assisted hatching pipettes. For the most part these functioned as well as the hatching pipettes, although the long thin taper made them even more fragile and therefore difficult to work with. Those not broken while trying to lineup the substrate would break after several uses from the pressure in the syringe.

The syringe – micropipette assembly was then held in place with a magnetic stage on top of an optical table. An x-y-z translation stage was bolted to the magnetic stage with the vertical adjustment control attached to a Newport Motion Controller digital micrometer. This allowed for very smooth alignments as well as precise jog increments to be made during experimental runs. A 360-degree rotational stage was then attached to the vertical surface of the three dimensional stage to control the angle of the tip of the micropipette. A third stage on a motorized track was used to move the substrate under the pipette tip as the polymer was dispensed to draw the waveguides. The motor has a variable speed control attached for adjustments in speed of the stage. By varying the speed of the stage, the thickness of the polymer line could be adjusted.

The waveguide was then cured under a UVP Blak-Ray longwave UV lamp. This allowed us to cure the polymer of the entire waveguide very quickly without an expensive laser or time intensive focusing issues.

3.2 The Polymer and Substrate

The two types of polymer for the core of the waveguides that were tested are Summers Optical type P-92 and type SK-9 optical cements. SK-9 is a

Acrylate/Methacrylate based polymer while P-92 is an Acrylate Monomer/Organic Di-Valent Sulfur Compound polymer. Although the company withholds actual chemical composition as proprietary information, it is enough to know that these are organic polymers. They are both UV cured photopolymers with practically no shrinkage during the curing process. These polymers were selected because they are traditionally used in optics as sealants or between optical elements since they are highly transparent. The viscosities of the two types of polymer are 900 - 1,400 cP for P-92 and 80 – 100 cP for SK-9. During initial attempts at drawing the waveguides, the SK-9 polymer was found to bead up too quickly, so the P-92 was the polymer used in the final waveguides for this project. The higher viscosity of the P-92 polymer allowed for drawing the waveguides with the tip of the micropipette above the glass substrate.

The wettability of the polymer to the surface of the substrate is another factor in the shape of the resulting waveguides. As seen in Figure 3, the contact angle, θ , of a liquid in contact with a solid is the angle tangent to the liquid at the point of contact with the solid surface. If the contact angle is large, the ratio of the width to the height of a drop of liquid will be smaller than if the contact angle is small.¹⁰

The ratio of width to height of drops of the P-92 polymer on the glass were measured by first cleaning the glass surface with acetone and dispensing drops of approximately 0.1 cc directly from the container onto the clean glass. The drops were allowed to settle for about two hours to reach equilibrium and were then cured. The ratio was found to be on the order of 20:1.



Figure 3: Diagram of the wetting angle θ

This ratio could be changed if the glass is treated differently before the droplet is deposited. For example, it was found that if the glass was simply cleaned with methanol instead of acetone before dispensing the drops, they had a much smaller radius and larger height measurements for the same approximate 0.1cc volume. The resulting ratio was much smaller, calculated to be between 6.0 and 6.5.

Drops of less than 10^{-4} cc were also investigated. Table 1 shows the results of these smaller size drops and how they depend on the time the polymer was allowed to settle. Although within the parameters we tested there seems to be no clear trend one can conclude that in the approach to equilibrium for small drops microscopic effects could take varying amounts of time to affect the drops. More tests would be needed to confirm any trend as more than suggestion. The Laplace equation for the curvature of the drop is given by¹⁰

$$P_L^Q - P_V^Q = \sigma_{LV} \left(\frac{1}{R_1} + \frac{1}{R_2} \right) \quad , \quad (2.1)$$

where P_L^Q and P_V^Q are the pressures on the liquid and vapor sides of the surface and R_1 and R_2 are the principal radii at a point Q. For sufficiently small drops gravity does not play a part in the shaping of the drop and the uniform surface tension results in R_1 and R_2 being equal and therefore the drops have a spherical surface. Because of this we expect a circular profile of the waveguides in two dimensions. For the 10^{-4} cc drops gravity can be ignored.¹¹ The contact angle can be calculated and are also listed in Table 1.

Table 1

Width (mm)	Height (mm)	w/h	Angle	Time
0.437	0.030	14.6	27	1.5 hours
0.288	0.017	16.9	24	1.5 min
0.338	0.052	6.5	60	1 min
0.300	0.045	6.7	58	.5 min
0.500	0.052	9.6	41	0 min

A second polymer is used for the cladding of the waveguide. There are many optical polymers available in a wide range of refractive indices. This allows for the adjustment of the cladding refractive index to get the optical properties needed at a given wavelength for a specific application. The only limiting quality of a polymer would be that the chemical make-up must not dissolve the waveguide it is placed over.

The substrate used is an optical flat made of fused silica with an index of refraction of 1.46. The index of refraction of the substrate will change some of the optical properties of the final waveguide. Other possible substrates include different types of glass, crystal, or even a flexible strip of polymer. Although it is possible to change the substrate to get a different index of refraction, a different material could have an effect on the shape of the waveguide due to different contact angles of the polymer on the substrate. The fused silica was used throughout this project to be consistent in the contact angle.

3.3 Fabrication of the waveguides

The first step in fabrication of the waveguides was to fill the tip of the micropipette. A small amount of the polymer was put into a 10 ml beaker and the tip of the micropipette was lowered into the polymer using the digital micrometer. Best results were achieved when the polymer was as fresh as possible out of the plastic bottle so only enough to cover the tip of the micropipette was used each time. Polymer left to sit exposed to the air for extended periods, even when shielded from light, exhibited composition changes that led to uneven waveguides.

Approximately 2.3 A of current was used to heat the syringe and cause the pressure to push the air out of the micropipette. Placing the tip into the polymer and watching the bubbles formed helped evaluate the amount of air that had evacuated. After air bubbles from the tip started to appear the current was left on for another 90-120 seconds. The current was then turned off and the syringe was allowed to cool, lowering the pressure and filling the micropipette with the polymer. This was the best timing to get enough of the polymer to fabricate the waveguide, but to not leave too much polymer or spend extra time waiting for the waste to be dispensed to clean the tip of the micropipette.

The UV light needed a few minutes to warm up and was turned on before the micropipette was adjusted into place to draw the waveguide. This minimized the shifting of the polymer by ensuring the curing process on the newly drawn waveguide was started immediately after being placed under the UV source.

After the syringe had completely cooled the micropipette tip was raised out of the beaker of polymer and the angle of the syringe was adjusted to 60 degrees from normal to the substrate on the rotating stage. Changes in the dispensing of the polymer were seen in adjustments of this angle within ten degrees either way. When the angle was lowered to 50 degrees or less, the tip was up too straight and would leave drops behind rather than a steady flow of the polymer in a cylinder to just be laid flat. By comparison when the angle was increased to 70 degrees the tip wicked too much of the polymer behind it and caused uneven pools to occur in the waveguide.

The glass substrate was placed on the motorized stage and was adjusted to place the tip very close to one end. The stage was then set to a speed of 2 cm per minute. Watching the movement of the micropipette tip through a stereoscope and using the digital micrometer the tip was lowered until it was just above the glass substrate. The current supply was set to 2.3 A and turned on. When the polymer could be seen extruding from the tip of the micropipette, it was lowered further until the polymer just touched the surface and the tip was still above the glass, the motorized stage was turned on, and the polymer was dispensed the length of the substrate. This method of the final setting of the tip occurring after the polymer had begun to appear at the tip did cause a larger drop at the beginning of the waveguide, but this wider part of the waveguide would be removed with the cutting and polishing of the end of the waveguide. Allowing the polymer to start before the final placement of the tip allowed the tip to be set at a height that the polymer would lay evenly on the glass but the tip

itself would not drag across the glass. Finally, as soon as the pipette cleared the far edge of the glass and the waveguide was complete, the substrate was placed under the UV light to cure.

The speed of the motorized stage determined the volume per length of the polymer being dispensed. This speed was used to control the width of the waveguides. However, there were limitations. If the variable speed was set too fast the surface tension of the polymer could not hold together and the waveguide would be broken. The low-end limitation of the speed of drawing the waveguides was the step motor for the motorized stage. The motion of the motor and therefore the stage were no longer smooth but jerky due to the step function motor. This resulted in a very obvious scalloped bottom edge to the waveguides from the starting and stopping of the motor. This probably did not continue to the top of the waveguides but made very dramatic angles at the base that were considered an unacceptable feature.

As mentioned before the UV light needed to be warmed up to ensure curing of the waveguide started as soon as possible after the last of the polymer was drawn out. If the waveguide was allowed to sit for too long before curing, it would pull apart and become droplets in a line. The points where variations in the line minimized the width seemed to be the most likely places for a break to occur. This effect was greater with the lower viscosity polymer. The beginning of the waveguide would start to degrade while the pipette was still depositing the end of the waveguide. When the more viscous P-92 was used, the waveguide stayed together long enough to get more length out of a draw of polymer.

The waveguide was sufficiently cured to observe under the microscope within 10 minutes, but full curing of the polymer took an hour in order to guarantee the waveguide did not deform over time. After the full curing time a cladding polymer would be added across the top of the cured waveguides and the whole system would be cured again.

The entire process of creating a waveguide that was fully cured took about an hour and a half. Most of the waveguides were inspected after the 10-minute pre-cure time and then placed back under the lamp to finish curing.

Several tries at different methods of polishing were attempted in an attempt to get the waveguide's attenuation coefficient. First polishing films with particles from .01 - 1 μ were tried. The thin pads and hard surface of the polishing table caused the polishing material to scratch the polymer or embedded themselves into polymer. A hand polishing technique was attempted next using wax that would help hold the crystals and be softer than the polymer to help keep the pressure be even. Sapphire powders varying in size from 1 μ to .05 μ were used. This was not an easy art to master and yielded almost no results. Finally velvet polishing pads with the same sapphire crystals were used on the polishing table again. This did yield some results but not good enough to couple light into, and extended time on the polishing table caused the polymer to be pulled away from the glass of the powder to get embedded between them. Further work would involve mastering the art of polishing polymers to allow transmission measurements to be taken and losses to be determined.

CHAPTER FOUR

RESULTS AND CALCULATIONS

4.1 *Waveguide characterization*

The waveguides produced using the above fabrication technique were reproducible between 12 – 20 microns wide and consistent for over 2 cm in length. Figure 4 shows a section of a 1.7cm long, 16 micron wide waveguide as seen with a scanning electron microscope. The small amount of roughness seen at the base of the waveguide does not affect the smoothness of the sides along the whole of the waveguide. The 3-dimensional profile measured with an atomic force microscope in Figure 5 of the same waveguide confirms the sides are smooth all along the length. The AFM profile also measured the height of the waveguide to be ~0.8 microns and the width to be 16 microns. This profile will be used for all further calculations of the properties of these waveguides.

Using the profile data provided by the AFM, points along the profile were plotted and a least squares fit to the profile was calculated. Figure 6 shows the best fit to a circular profile and can be expressed as

$$t(x) = -38.5 + \sqrt{(39.4)^2 - (x)^2} \quad (4.1)$$

where x is the displacement from the center of the waveguide in microns and t is the height at any point x . This equation is then used to find the effective index of refraction for the waveguide.

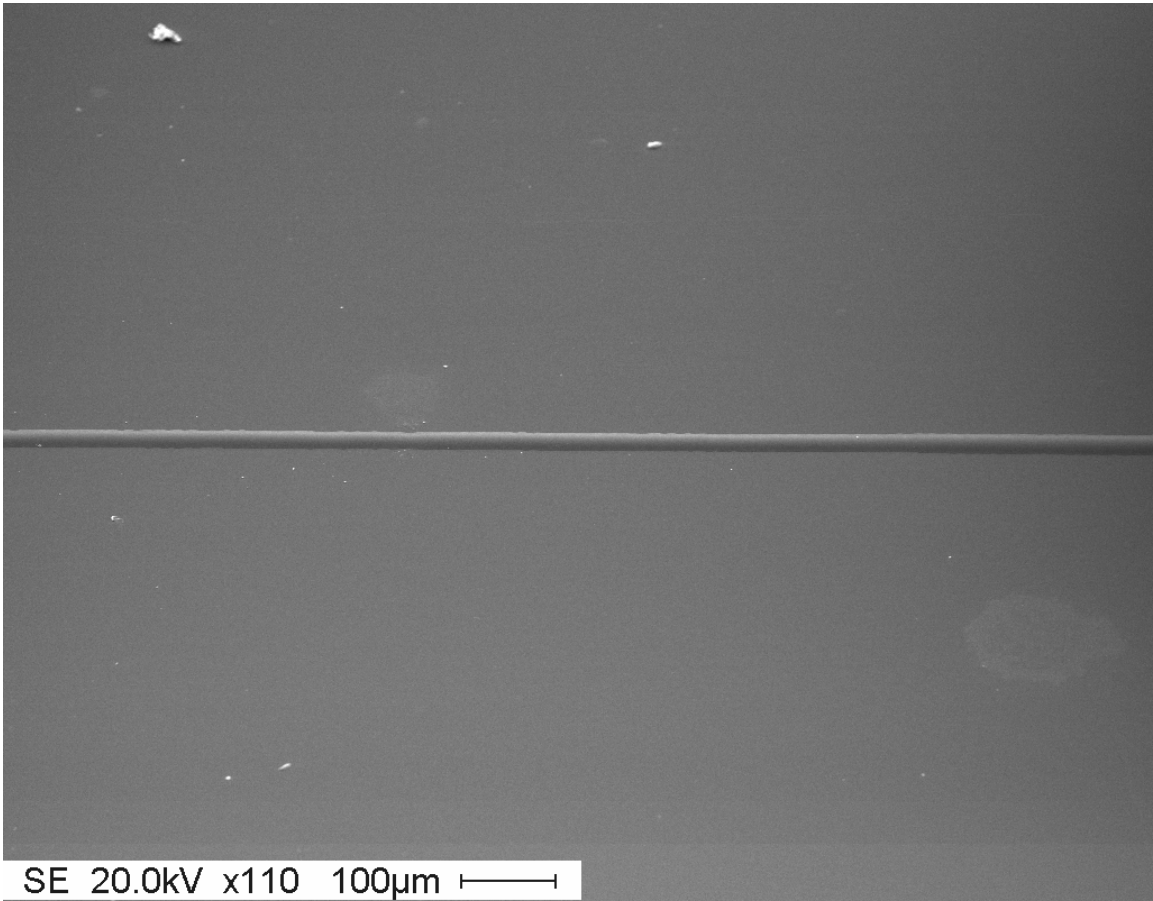


Figure 4: 1.7cm Segment of waveguide as seen with a Scanning electron microscope

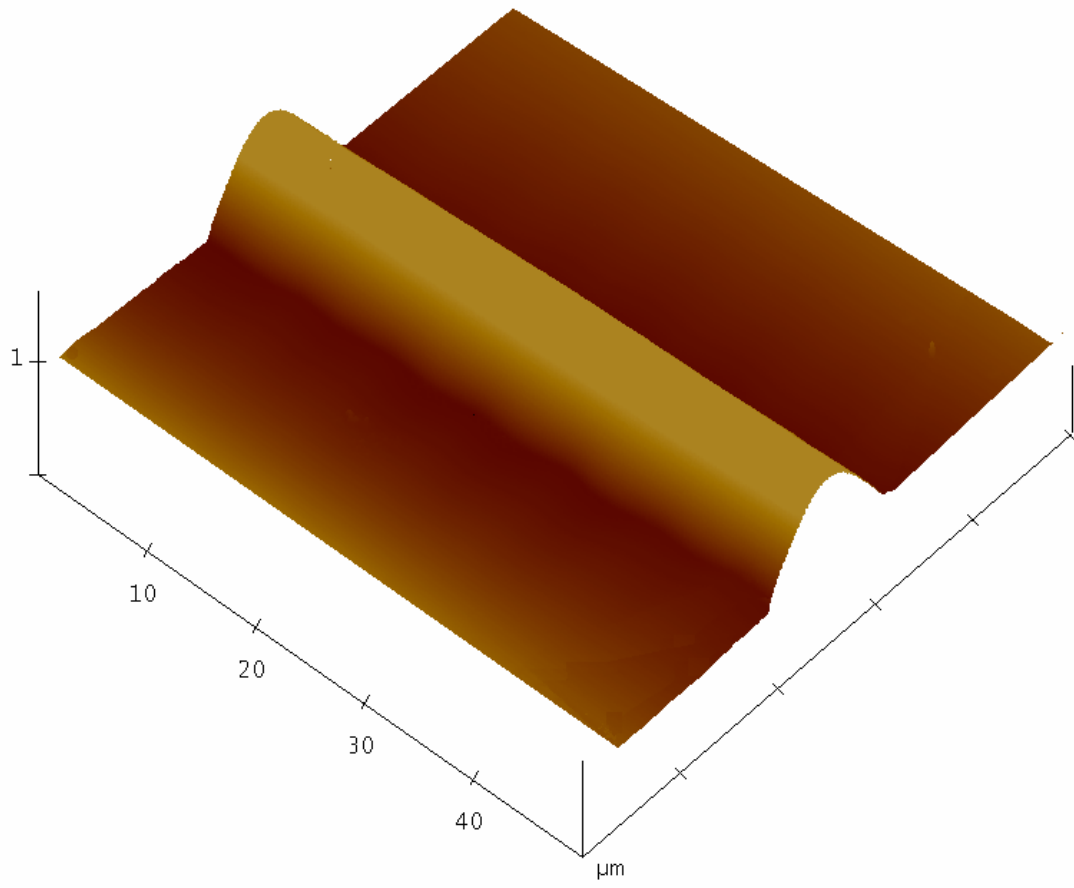


Figure 5: 3-Dimensional scan taken with an atomic force microscope.

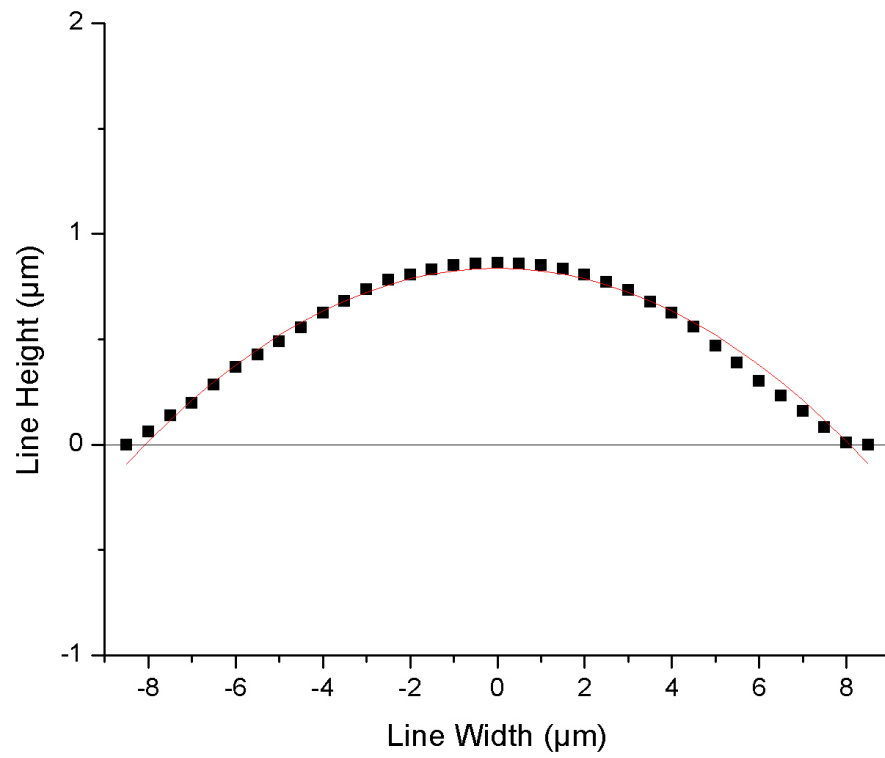


Figure 6: Best circular fit to profile data from atomic force microscope

4.2 The Effective Index of Refraction

Once the waveguide dimensions have been determined, the properties of the waveguide can be calculated. Ideally this would be done in two dimensions. Since this would be quite difficult, the problem was treated as two orthogonal planar waveguides instead. The refractive index of the core polymer is $n_2 = 1.51$ and of the substrate $n_1 = 1.46$, as noted in section 3.2. Finally to achieve the optical properties in this thesis project a cladding polymer of $n_3 = 1.48$ will be used throughout the calculations.

4.2.1 Theory and Derivation of Effective Index of Refraction Equations for TE Modes

The mode profile of the waveguide can be calculated approximately by first finding the effective index for a slab dielectric waveguide consisting of a film of thickness t and index of refraction n_2 with a substrate and cladding of refractive indices n_1 and n_3 respectively, where $n_1 < n_3 < n_2$ for each position x along the bottom of the waveguide. This effectively breaks the circularly shaped waveguide into a series of planar waveguides. Figure 7 defines the 3-dimensional axis used in this system. Similar to the method used by Keyworth, et al. the assumption is made that the waveguide satisfies the scalar wave equation⁸

$$\frac{\partial^2 E}{\partial x^2} + \frac{\partial^2 E}{\partial y^2} + \frac{\partial^2 E}{\partial z^2} + n^2(x, y)k_0^2 E(x, y, z) = 0, \quad (4.2)$$

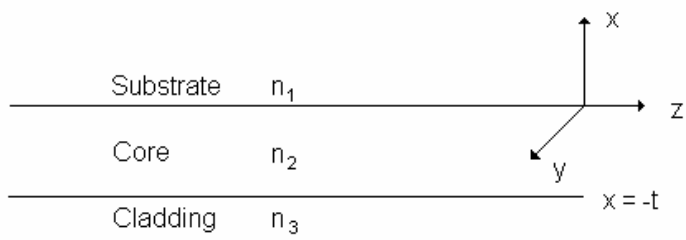


Figure 7: Diagram of the Planer Waveguide Coordinate system

where k_0 is the wavenumber given by

$$k_0 = \frac{2p}{l}, \quad (4.3)$$

and l is the wavelength of light in a vacuum. For each displacement from the center of the waveguide, x , the guided field is expanded in terms of a set of M local guided asymmetric slab waveguide modes as

$$e(x, y, z) = \sum_m^M E_m(y, z) S_m(x) e^{-j\mathbf{b}_m z}, \quad (4.4)$$

where $S_m(x)$ are orthogonal function of the form

$$S_m(x) = C \begin{cases} e^{-qx} & 0 \leq x < \infty \\ \cos(hx) - \frac{q}{h} \sin(hx) & -t \leq x \leq 0 \\ \left(\cos(ht) + \frac{q}{h} \sin(ht) \right) e^{p(x+t)} & -\infty < x < -t \end{cases}, \quad (4.5)$$

and h , q , and p are given by

$$h = \sqrt{n_2^2 k^2 - \mathbf{b}^2}, \quad (4.6)$$

$$q = \sqrt{\mathbf{b}^2 - n_1^2 k^2}, \quad (4.7)$$

$$p = \sqrt{\mathbf{b}^2 - n_3^2 k^2}. \quad (4.8)$$

After imposing continuity conditions, Equation (4.5) yields

$$\tan(ht) = \frac{h(q+p)}{h^2 - pq}, \quad (4.9)$$

which can be solved for the propagation constant \mathbf{b} .^{8,12} The effective index of refraction for each slab waveguide of thickness t is then calculated by substituting \mathbf{b} into

$$n_{eff}^2 = n_2^2 - \frac{n_2^2 k^2 - \mathbf{b}^2}{k^2}. \quad (4.10)$$

Finally when the effective index n_{eff} , for each of our different slab waveguides is plotted versus each displacement from the center, x , and a parabolic fit is made to the curve, the equation will be used to provide a parabolic index profile for the horizontal direction.^{8, 12}

In the symmetric case of $n_3 = n_1$ there would always be at least one mode, since $p = q$ and the denominator of equation (4.9) would equal zero. However, when $n_3 \neq n_1$ guided modes exist only for sufficiently thick core. This limit occurs when \mathbf{b} causes equation (4.6), (4.7), or (4.8) to no longer be a real number. Therefore, since $kn_1 < kn_3 < \beta < kn_2$, kn_2 and kn_3 are the limits in this case. Figure 8 shows the dispersion curves for the only confined TE mode of the waveguide for the assumed conditions.¹²

4.2.2 Calculations of the Parabolic Profile Graded Index of Refraction

At each given I the calculation of the effective index of refraction for a thickness of the waveguide was done with the computer program written in the C programming language given in Appendix 1. Equation (4.1) was used to approximate the thickness at different x displacements along the width and the result was substituted into Equation (4.9). The right side of Equation (4.9) was

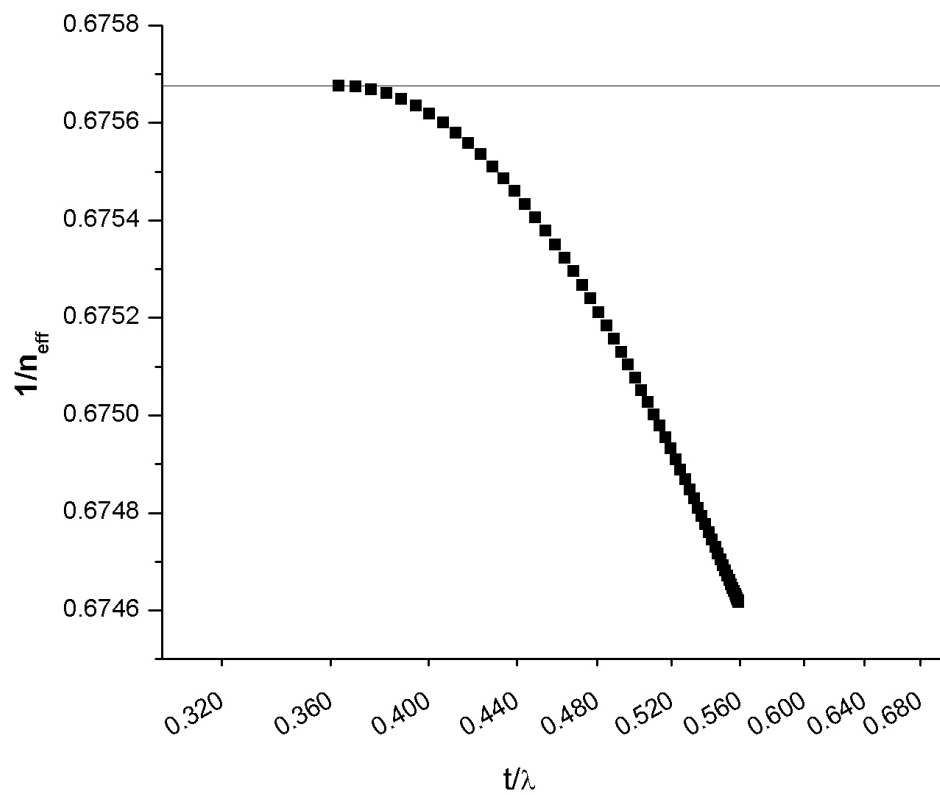


Figure 8: Dispersion curve for the confined mode for 1.50μ wavelength with a cladding index of 1.48 and a core index of 1.51.

subtracted from the left side and the program varied b until the difference between the left and right sides of the equation was less than .009. This solution of b was then substituted into equation (4.10) and the effective index of refraction for each thickness was found and written to a file.

When these n_{eff} points were plotted versus their displacements from the center, the points marked by squares in Figure 9 were obtained. For this profile $I = 1.50$ microns, a typical telecommunications wavelength, was used. The polynomial curve shown in Figure 9 was found by first fitting a line to the plot of y versus x where

$$y = \sqrt{\Delta n_{eff}(x)}, \quad \text{and} \quad \Delta n_{eff}(x) = n_{eff}(0) - n_{eff}(x). \quad (4.11)$$

The square of the slope of this linear graph was then used as the coefficient of x^2 in the equation of parabola for the effective index of refraction is given by

$$n(x) = 1.48232 - (1.19 \times 10^{-2})^2 x^2. \quad (4.12)$$

There is some error in the approximation at the outer edges of the waveguide. This error is negligible since the spot size is small compared to the width of the waveguide.

No higher TE modes were found by the program for this wavelength. This corresponds with the boundary condition of the dispersion curve in Figure 8. For a mode to exist $\beta > n_3 k$ for a given t . If $\beta = n_3 k$ then $p = 0$, and equation (4.9) becomes

$$\tan(ht) = \frac{q}{h}, \quad (4.13)$$

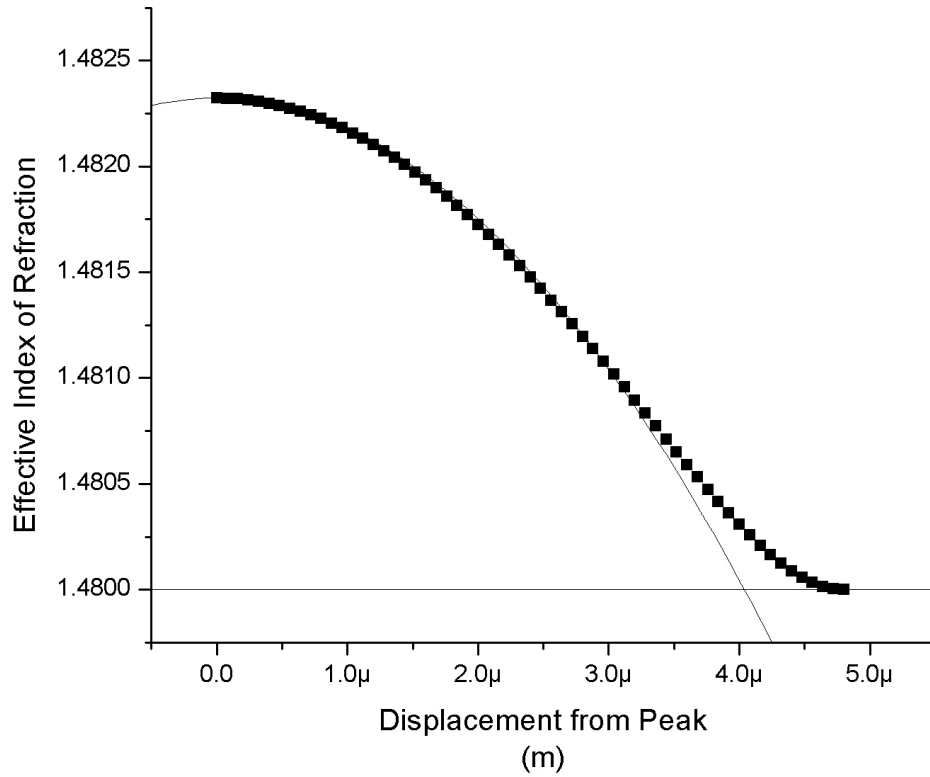


Figure 9: Graph of effective index of refraction for 1.50 μ and parabola approximation of the profile to show fit.

This allows us to find the minimum thickness to support modes. The waveguides are of the correct thickness to support one mode and only one mode.

4.2.3 Calculations for the TM modes

The TM mode approximation was done with the same method as the TE modes. For the TM modes however, the eigenvalue equation changes to

$$\tan(ht) = \frac{h(\bar{q} + \bar{p})}{h^2 - \bar{p}\bar{q}} \quad , \quad (4.14)$$

where

$$\bar{p} \equiv \frac{n_2^2}{n_3^2} p \quad , \quad (4.15)$$

$$\bar{q} = \frac{n_2^2}{n_1^2} q \quad . \quad (4.16)$$

This approximation resulted in no TM modes. ¹²

4.3 Single mode waveguide determination

With the approximation of the parabolic profile of the graded index of refraction the number of modes can now be estimated using the method of calculating modes in a graded index fiber. For this portion of calculation the fiber geometry, instead of the planar geometry, was used because of the availability of the needed formulas. This is an oversimplification of the problem, but offers a quick semi-quantitative answer. The fiber is described as having a cylindrical core of radius r .

4.3.1 Theory for Determining the Number of Modes

Guided rays in a graded index fiber follow oscillatory trajectories. Within fibers these trajectories are helical and are confined within two cylindrical shells of radii r_l and R_l , where $0 \leq r_l < R_l \leq r$, and r is the radius of the fiber as shown in Figure 10.

The region bound by r_l and R_l occurs for the values for r where the wavevector portion of the Helmholtz equation given by

$$k_r^2 = n^2(r)k_0^2 - \mathbf{b}^2 - \frac{l^2}{r^2} \quad , \quad (4.17)$$

is real. Here $n(r)$ is the profile equation, k_0 is the wavenumber at a given frequency, r is the radial position and l , like \mathbf{b} is a ray invariant in the k_θ direction and contributes to the helical component of the ray down the fiber as shown in Figure 10.

Because the minimum and maximum refractive index values are similar the critical angles are very large and each ray propagates nearly parallel to the axis of the waveguide and is known as the paraxial approximation. This allows for use of the power law function stated as

$$n^2(r) = n_2^2 \left[1 - 2 \left(\frac{r}{\mathbf{r}} \right)^s \Delta \right] \quad , \quad (4.18)$$

where

$$\Delta = \frac{n_2^2 - n_3^2}{2n_2^2} \quad , \quad (4.19)$$

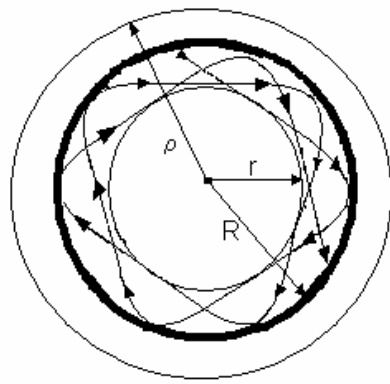


Figure10: Helical path of rays in a graded index fiber

and g here is the grade profile parameter. This parameter determines the steepness of the profile. If the profile is linear $g = 1$ and at $g = 2$ it is quadratic. As g approaches ∞ , the graded index approaches the step function. The waveguides in this work have a parabolic graded index, so $g = 2$ will be substituted into equation (4.18).^{1, 13}

To find the wavelengths for which the waveguide has at least one mode, the condition that the wave must reproduce itself after one helical period will be used. This occurs when the radial round trip path length corresponds to a phase shift in the wavevector k_r of a multiple of 2π , or

$$2 \int_{r_i}^{R_l} k_r dr = 2\pi m, \quad m = 1, 2, \dots \quad (4.20)$$

Thus for a given wavelength the number of modes is equal to the integral in equation (4.20) rounded down to the next closest integer. This must then be determined for each integer l to determine the number of modes. If a given integer of l has zero modes, then no greater value of l will produce modes. Therefore to show a single mode waveguide only the $l = 0$ and $l = 1$ cases need to be addressed.¹³

4.3.2 Calculation of wavelengths that have only one mode

To show the waveguides in this study are single mode for a given range of wavelengths equation (4.20) must first be solved for the case of $l = 0$. Because k_r is the helical component of the wavevector equation, an l of zero results in a

meridional wave. Also $\mathbf{b}^2 = n_2^2 k^2$ is used to maximize the range of possible r -values. The phase shift now becomes

$$2 \int_{r_i}^{R_l} k_r dr = 2 \int_{r_i}^{R_l} \sqrt{n^2(r)k^2 - \mathbf{b}^2} dr, \quad (4.21)$$

and when the integral is solved, gives the equation

$$2 \int_{r_i}^{R_l} k_r dr = \mathbf{p}^2 n_2 \sqrt{2\Delta} \frac{\mathbf{r}}{\mathbf{l}} \quad (4.22)$$

Figure 11 shows the solutions for equation (4.21) versus \mathbf{l} . The wavelengths ranging from 1.2 - 1.5 microns have solutions between 2π and 4π , and therefore have only one mode for the $l = 0$ case.

The integral of the phase shift for the $l > 0$ cases

$$2 \int_{r_i}^{R_l} \sqrt{n^2(r)k^2 - \mathbf{b}^2 - \frac{l^2}{r^2}} dr = 2\mathbf{p}m, \quad (4.23)$$

is much more complicated. Using a u substitution for r^2 , and adjusting the limits of integration, equation (4.23) now takes the form

$$\int_{r_i^2}^{R_l^2} \frac{\sqrt{a + bu + cu^2}}{u} du = 2\mathbf{p}m, \quad (4.24)$$

where

$$a = l^2, \quad (4.25)$$

$$b = (n_1^2 - n_2^2)k_0^2, \quad (4.26)$$

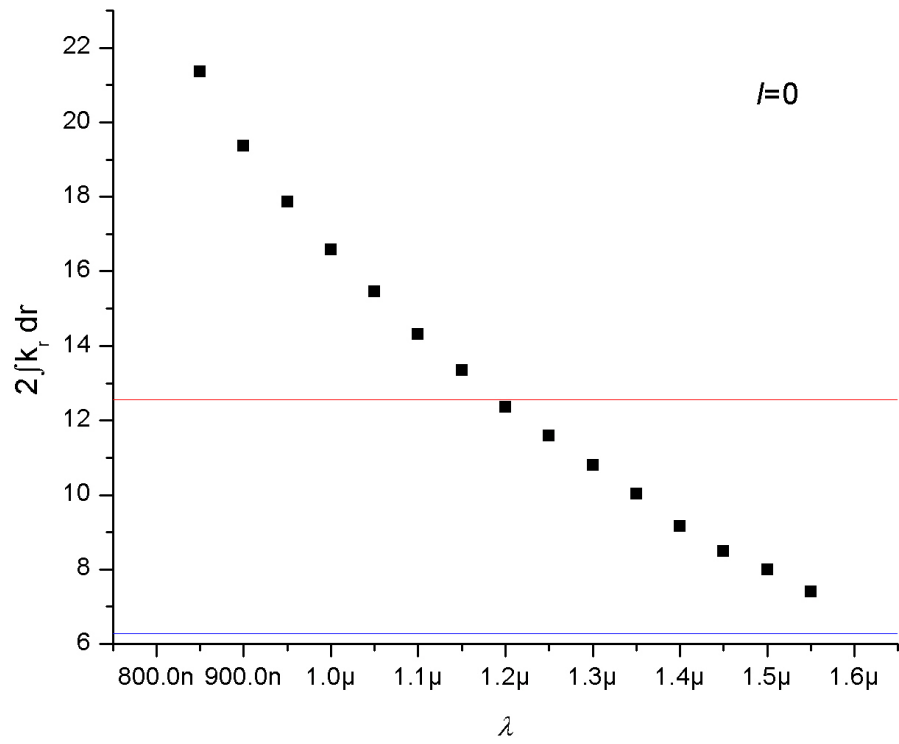


Figure 11: $2\int k_r dr$ vs. λ - for $l = 0$; Region of Only One Mode

Wavelengths with only one mode fall within the region marked by the 2π and 4π lines

$$c = \frac{-n_1^2 k^2 2\Delta}{r}, \quad (4.27)$$

and the solution to the indefinite integral gives¹⁴

$$\frac{\left[2\sqrt{c} \ln\left(\frac{4ac - b^2 - b\sqrt{b^2 - 4ac}}{b + \sqrt{b^2 - 4ac}}\right) \sqrt{a} - b \ln\left(-\frac{\sqrt{b^2 - 4ac}}{\sqrt{a}}\right) - 2\sqrt{c} \ln\left(\frac{4ac - b^2 + b\sqrt{b^2 - 4ac}}{b - \sqrt{b^2 - 4ac}}\right) \sqrt{a} + b \ln\left(-\frac{\sqrt{b^2 - 4ac}}{\sqrt{a}}\right) \right]}{2\sqrt{a}} \quad (4.28)$$

This solution is again plotted versus l and the resulting graph is shown in Figure 12. This shows the later part of the range that previously had only one mode for the $l = 0$ case has no modes for the $l = 1$ case. This is the range for which the waveguide with a cladding index of refraction of 1.48 is only able to support a single mode.

4.4 Results for claddings with a different index of refraction

As noted in section 3.2 a polymer of any index of refraction less than the refractive index of the core polymer could be used as cladding for this waveguide. The previous calculations were carried out for other refractive indices, but did not yield single-mode results in a wavelength range that was as desirable as the $n_2 = 1.48$ that was used.

An index of refraction of 1.47 for the cladding resulted in wavelengths of 1.55 microns or less having solutions to equation (4.20) greater than 4π for the case of $l = 0$. These waveguides would have a minimum of two modes just in the meridional plane. Brief calculations for a cladding with refractive index of 1.50 were also performed. The longest wavelength to support a mode was less than

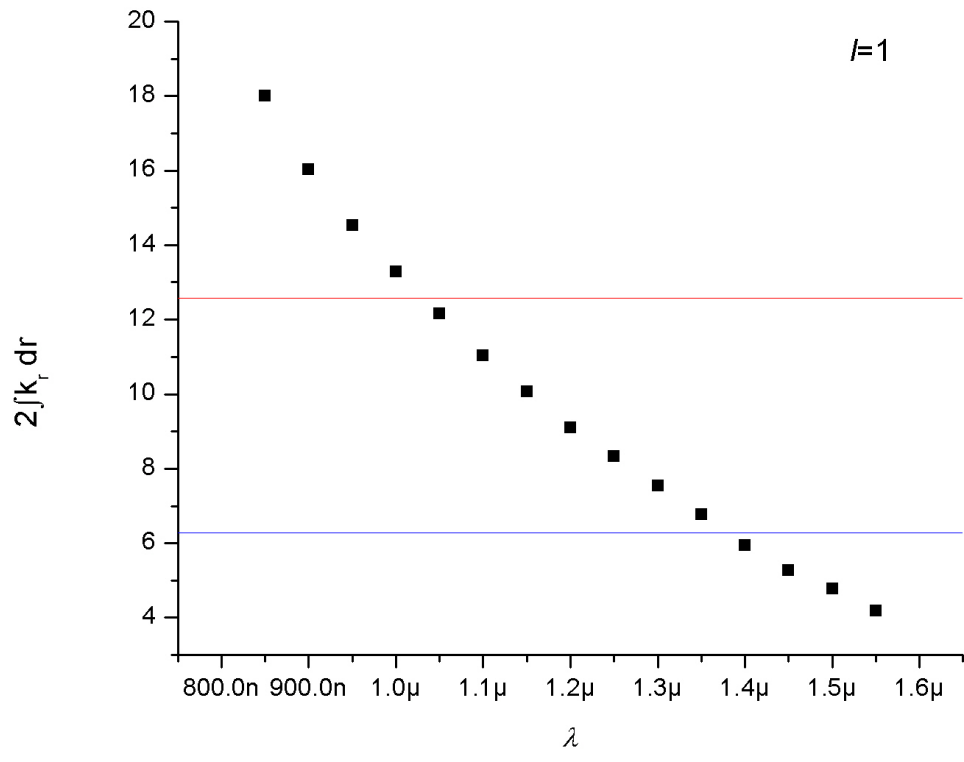


Figure 12: $2\int k_r dr$ vs. λ - for $l = 1$; Regions With No Modes at $l = 0$

The region of wavelengths below 2π have only the modes from the $l = 0$ case

0.7 microns for this cladding. This would make the range for single mode wavelengths much lower than desirable.

4.5 Spot Size Calculations

The spot sizes were estimated to find what the shape of the beam would be when coupling into and out of the waveguides. The spot size is defined as the radius of a Gaussian beam where the field is $1/e$.⁸ The electric field of a parabolic graded-profile planar waveguide is proportional to

$$e^{\left(\begin{array}{c} V \frac{x^2}{r^2} \\ -\frac{r^2}{2} \end{array} \right)} \quad (4.29)$$

where

$$V = \frac{2pr}{l} \sqrt{n_2^2 - n_3^2} . \quad (4.30)$$

Thus

$$w_x = \sqrt{\frac{2}{V}} r , \quad (4.31)$$

is the spot size along the x-axis.¹³

The spot size, w_y , for the y-axis is solved similarly for the Gaussian beam.

This results in the spot size equation¹³

$$w_y = \frac{\cos\left(\frac{ht}{2}\right) + \frac{q}{h} \sin\left(\frac{ht}{2}\right)}{e}. \quad (4.32)$$

Figure 13 shows the calculated spot sizes for both the x, plotted as squares and y, plotted as circles, axes of the beam versus wavelength. The ratio of the width of the spot size to the height varies from 2 to 4 for the .850 – 1.50 micron wavelength range. This is a much better ratio for the coupling of light into the waveguide than the width to height ratio of 20 for the waveguide itself.

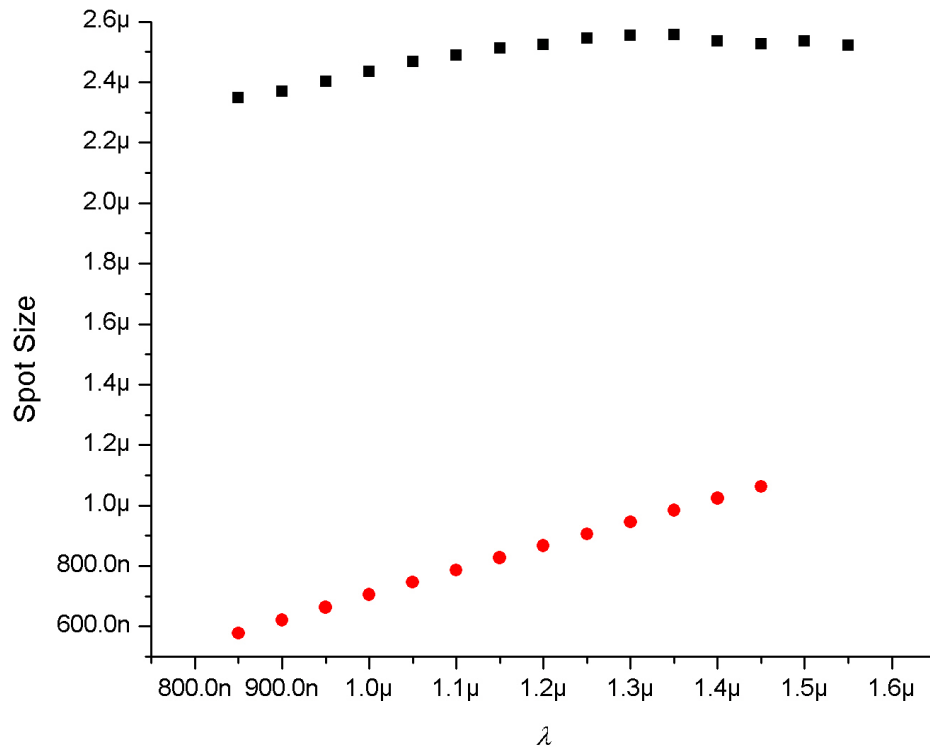


Figure 13: Spot Sizes in both the x , squares, and y , circles, axis.

CHAPTER FIVE

CONCLUSION

5.1 *Summary*

This project successfully demonstrated that dispensed polymer single-mode waveguides could be created with a biological micropipette. This fabrication process used an organic optical cement polymer from Summers Optical dispensed from a biological micropipette from Humagen Diagnostics. The polymer was dispensed onto a glass substrate guided under the pipette with a translational stage and was cured under an inexpensive UV lamp. The size of the waveguides was reduced to 15 – 20 microns across and 0.8 microns high from that in previous work in which dispensed polymer waveguides from a 160 micron tip of a syringe were on the order of 300 microns wide. A computer program to solve for the effective index at any point on the waveguide profile was developed to determine the profile of the graded index waveguides. The index variation was shown to be parabolic. Calculations using the graded index of refraction profile confirmed the waveguides were sufficiently small to support only one mode in the telecommunication range of wavelengths from 0.8 – 1.55 microns. Finally, the spot sizes of these waveguides were shown to be within coupling standards implying reasonable losses when coupled to other devices.

This work showed the ease of creating these waveguides with significantly less expense than other waveguide fabrication techniques. Minimal equipment is needed and the results are easily reproduced. Research and development of new applications should become significantly quicker, less expensive and, as indicated by the theoretical calculations, extremely versatile. This new method holds much promise for the field of photonics and its applications.

5.2 Future Work

The next step for future research on this project would be to confirm the approximate results calculated above. This was not within the scope of this thesis project because learning the art of polishing polymer takes time and was not completed within the time constraints. The polymers require special attention compared to crystals or glass because they are softer and scratch more easily.

Work in this field could continue with the development of active devices, such as optical amplifiers by adding a dopant to the polymer used for these waveguides. Another aspect not covered in this study would be the addition of other waveguides to create splitters or coupling devices. As noted in previous chapters, optical properties could be adjusted by adjusting the polymer used for the cladding, core or the material for the substrate. With the features of these waveguides being single-mode and still having the versatility of being constructed of polymer, these waveguides have endless possibilities.

References

1. B.E. A. Saleah, and M. C. Teich, *Fundamentals of Photonics* New York: Wiley-Interscience, 1991,
2. W. H. Steier, et al., "Polymer Electro-optic Devices for Integrated Optics," *Chemical Physics*, vol. 245, pp. 487-506, 1999
3. G. Karve, B. Bihari, R. T. Chen, "Demonstration of optical gain at 1.06 μm in a neodymium-doped polyimide waveguide," *Applied Physics Letters*, vol. 77, pp. 1253-1255, 2000
4. C. Darraud-Taupiac, V. Binsangou, J. L. Decossas, J. C. Vareille, "Optical Waveguides Fabricated on Polymer Substrate By Electron Beam," *Materials Science in Semiconductor Processing*, vol. 3, pp. 363-365, 2000
5. A. Neyer, T. Knoche, L. Müller, "Fabricaion of Low Loss Polymer Waveguides Using Injection Moulding Technology," *Electronics Leters*, vol. 29, pp. 399-401, 1993
6. J. Koo, P. G. R. Smith, R. B. Williams, C. Riziotis, M. C. Grossel, "UV Written Waveguides using Crosslinkable PMMA-based copolymers," *Optical Materials*, vol. 23, pp. 583-592, 2003
7. B. P. Keyworth, J. N. McMullin, R. Narendra, I. R. MacDonald, "Computer-Controlled Pressure-Dispensed Multimode Polymer Waveguides," *IEEE Transactions on Components, Packaging and Manufacturing Technology – Part B.*, vol. 18, pp. 572 – 577, 1995
8. D. W. Boertjes, J. N. McMullin, B. P. Keyworth, "Graded Effective Index Planar Polymer Waveguides," *Journal of Lightwave Technology*, vol. 14, pp. 2714 – 2718, 1996
9. L. H. Slooff, et al, "Rare-earth doped polymers for planar optical amplifiers," *Journal of Applied Physics*, vol. 91, pp. 3955-3980, 2002
10. S. Wu, *Polymer Interface and Adhesion*, New York: Marcel Kekker, Inc.,1982
11. N. Eustathopoulos, M. G. Nicholas, B. Drevet, *Wettability at High Temperatures*, New York: Pergamon Materials Series,1999
12. A. Yariv, *Quantum Electronics*, New York: John Wiley & Sons, 1989, 3rd Edition

13. A. W. Snyder, J. D. Love, *Optical Waveguide Theory*, New York: Chapman and Hall, 1983

14. R. C. Weast, Ed., *Handbook of Chemistry and Physics*, Cleveland, Ohio: Chemical Rubber Co., 1971

APPENDICES

APPENDIX I

This is the C program referenced in Chapter 4, Section 4.2.2

```
/******  
/*      effindex.c          07/09/03  Last Updated: 09/02/03          */  
/*  Jill Kalajian          */  
/*      This program will use the equation for the shape of my lines of polymer          */  
/*      and will calculate the effective index of refraction and store it in a text          */  
/*      file.          */  
/******  
  
#include <stdio.h>  
#include <math.h>  
#include <stdlib.h>  
  
#define n1 1.46          /*      Index of Refraction for the glass substraight          */  
#define n2 1.51          /*      Index of Refraction for the polymer waveguide          */  
#define n3 1.475        /*      Index of Refraction for the polymer cladding          */  
#define k 2*3.14159/.000001550  /* Wave number */  
  
#define sqr(a) (a*a)  
  
main()  
{  
    FILE * outfile;  
    /* The output will be to a file that will be tab delimited so it can          */  
    /* then be read into MicroSoft's Excell or Microcal's Origin.          */  
  
    double x, t, h, p, q, b, diff, effind;  
    /* Variables :          */  
    /* x : x coordinate of the waveguide to find the height each time          */  
    /* t : height of the waveguide this will be calculated from each x          */  
    /*      coordinate.          */  
    /* h,p,q : the small equations substituted in the large equation to          */  
    /*      make seeing the equation easier. They are the same as the          */  
    /*      equations h, p, & q in Yariv          */  
    /* b : Beta from Yariv - this is what I will solve for and will then be          */  
    /*      used to calculate the effective index of refraction          */
```

```

/* diff: Variable to hold the difference between the two equations | */
/*      will consider b a solution to the equations when the      */
/*      difference is less than .009                               */
/* effind: Variable for the effective index calculation             */

outfile = fopen("eind-475-155.txt","w");
fprintf(outfile,"\teffind\t\t\tb\t\tsqrtdiff 1.55\n");
/* The output file is created and opened for writing.             */

effind = 0;
for (x = 0; x < .00000858; x = x + .00000008)
/* This loop will run for approximately 100 x coordinates of the width */
/* of the polymer. The height is calculated and then another loop will */
/* solve the two equations for b (Beta)                               */
{
    t = -.00003853655 + sqrt(sqrt(.00003937502) - sqrt(x));

    diff = 1.0;
    for (b = (k*n3); (diff > .009 || diff < -.009); b = b++)
/* This for loop will calculate both equations for each height and */
/* will change b till the difference in the equations is             */
/* approximitly 0. This is the intercept of the two equations      */
{
        p = sqrt(sqrt(b) - (sqrt(n3) * sqrt(k)));
        q = sqrt(sqrt(b) - (sqrt(n1) * sqrt(k)));
        h = sqrt(sqrt(n2) * sqrt(k) - sqrt(b));

        diff = (tan(t*h) - ((q+p)/(h-(q*p)/(h))));
    }

    effind = sqrt(sqrt(n2) - (sqrt(h)/sqrt(k)));

    /* Now write results of each effective index to a text file */
    fprintf(outfile,"% .10ft%.10ft%.10ft%.10ft\n",x,effind,t,b);
}
/* Close out put file */
fclose(outfile);
}
/* End of program */

```